Jahn-Teller effect on PrO_2: A multimode vibronic model

G. Bevilacqua
INFM and Dipartimento di Fisica, Università di Siena, Via Roma 56, 53100 Siena, Italy

D. Ippolito and L. Martinelli
INFM and Dipartimento di Fisica "E. Fermi," Via Buonarroti, 2, 56100 Pisa, Italy

(Received 5 December 2003; published 23 April 2004)

Recent well resolved neutron spectroscopy measurements of the magnetic excitations in PrO_2 provide evidence of the dynamical Jahn-Teller effect on this dioxide. We calculate the differential cross section in a wide range of energy and the magnetic moment of PrO_2 after the analysis of different vibronic models (one-mode and two-mode phonon coupling models) for electrons interacting with distortions of e and t_2 symmetry. The Lanczos-recursion procedure is followed to determine the vibronic states in a nonperturbative way and with high precision. A very convenient choice of the initial state of the Lanczos chain is suggested here so allowing easy calculation of the differential cross section. It is found that e modes do not give reliable results in terms of intensities of the expected transitions, while t_2 modes in a multimode vibronic model lead to a quite good agreement with the experimental measurements.

DOI: 10.1103/PhysRevB.69.155208 PACS number(s): 71.70.Ej, 76.30.Kg

I. INTRODUCTION

Among rare-earth dioxide, praseodymium dioxide has interested the researchers for its uncommon properties associated with Pr $4f$ electrons[2] and for a future possibility to be used to substitute SiO_2 in decanano MOSFET transistors.[3] At low temperature PrO_2 (antiferromagnet with Néel point at 14 K) has a magnetic moment anomalously small[4,5] when compared with the value expected for the ground electron-spin state in a cube crystal field; Pr^{4+} ions exist almost completely in a $4f^1$ configuration, now an ascertained opinion,[4,1] and Pr^{4+} ground state is orbitally degenerate. So it is natural to think of the possibility of interaction between the electron and ion motion or in other words of a dynamical Jahn-Teller (JT) effect. Actually well resolved magnetovibrational spectra recently obtained by Boothroyd and co-workers[1] provide experimental evidence of this theoretical expectation. In fact the experimental spectra exhibit at low energy two peaks separated by about 130 meV, a broad band (extending from 10 to 80 meV) centered at about 30 meV and a 160 meV shoulder. These observed behaviors cannot be explained in a scheme including only crystal-field and spin-orbit interactions, instead a JT coupling can produce a number of levels having electronic and vibrational character,[6] as found also by Boothroyd *et al.*[1] in a simplified model within a perturbative scheme.

In this paper we analyze in a more complete way, treating on the same footing crystal-field and spin-orbit interaction, different linear vibronic models, single-mode and two-mode phonon interaction models, consistent with the symmetry of the system under study. Actually a multimode interaction model is suggested by the appearance of the broad intermediate scattering band. Then we calculate the differential cross section and the magnetic moment.

The introduction of the electron-phonon interaction, in particular, the use of two-mode interaction models, requires handling matrices with a very large number of degrees of freedom. However, we consider linear interaction models leading to matrices in a sparse form, then the Lanczos-recursion procedure[8] can be successfully used. In the literature this method has been followed in solid-state physics in connection with electronic problems[9,10] or extended to dynamical JT problems, allowing a nonperturbative treatment of the absorption as well as luminescence spectra of localized impurity centers.[11–13] Also in this dioxide the electron orbital states of Pr^{4+} ions can be considered reasonably localized,[1] so cooperative effects can be neglected and the Lanczos-recursion method can be efficiently used to calculate the differential cross section and the magnetic moment, provided that the initial state of the iterative procedure is chosen in a proper way.

In Sec. II we discuss the model Hamiltonians used; in Sec. III we expose the calculation procedure; in Sec. IV we show the results obtained for the various models considered. Comments and conclusions are presented in Sec. V.

II. MODEL HAMILTONIAN

PrO_2 has a fluorite structure type, where Pr^{4+} ion is at the center of a cube whose vertices are occupied by eight O^{2-}. It has been shown[1] that the Pr^{4+} ion has one localized electron in the $4f$ configuration giving rise to a ground ^2F term 14 times degenerate including spin. This term is split by a cubic crystalline field into states having the symmetry of the representations Γ_{2u}, Γ_{4u}, and Γ_{5u} of the group O_h (notation of Koster[14]), as shown in the left side of Fig. 1. In the next the label u, indicating the symmetry to respect the inversion, will be understood. The spin-orbit interaction $\lambda(\mathbf{LS})$ produces the following set of levels:

$$|E_0\rangle_i = a_0|\Gamma_{8,i}\rangle + a_0'|\Gamma_{8,i}'\rangle, \quad i = -\frac{3}{2}, -\frac{1}{2}, \frac{1}{2}, \frac{3}{2},$$

$$|E_1\rangle_i = a_1|\Gamma_{7,i}\rangle + a_1'|\Gamma_{7,i}'\rangle, \quad i = -\frac{1}{2}, \frac{1}{2},$$

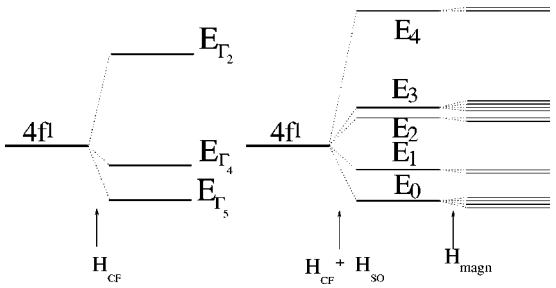

FIG. 1. Levels splitting produced by crystal field (left); crystal field, spin-orbit interaction, and local magnetic interaction (right).

$$|E_2\rangle_i = |\Gamma_{6,i}\rangle, \quad i = -\frac{1}{2}, \frac{1}{2},$$

$$|E_3\rangle_i = a_3|\Gamma_{8,i}\rangle + a_3'|\Gamma_{8,i}'\rangle, \quad i = -\frac{3}{2}, -\frac{1}{2}, \frac{1}{2}, \frac{3}{2},$$

$$|E_4\rangle_i = a_4|\Gamma_{7,i}\rangle + a_4'|\Gamma_{7,i}'\rangle, \quad i = -\frac{1}{2}, \frac{1}{2}. \tag{1}$$

Here i labels the rows of each double group representation. A molecular exchange field interaction $H_{magn} = g\mu_B \mathbf{H}\mathbf{J}$, representing a local effective magnetic interaction with the ordered magnetic moments, removes completely the degeneracy, as shown in the right part of Fig. 1.

We assume for the spin-orbit coupling constant the value $\lambda = 100.5$ meV as used in literature[1] and we fix at first the crystal-field parameters[7] F_4 and F_6 equal to 265.8 meV and 134.3 meV, respectively.[15] Then the energies of the five multiplets turn out to be $E_0 = 0$, $E_1 = 129$ meV, $E_2 = 337$ meV, $E_3 = 367$ meV, and $E_4 = 767$ meV (the ground electron state energy E_0 is chosen as reference energy). The energy separation produced by H_{magn} on the multiplets is of the order of 2–3 meV choosing $g\mu_B H = 0.5$ meV and $\mathbf{H}$ in the (1,1,1) direction.[1] Its evident result is that, within this simple interaction scheme, the experimental measurements cannot be justified, in particular, the experimental cross section in the range 0–160 meV.

It is well known that in presence of degeneracy (or quasidegeneracy) of molecular orbitals the Born-Oppenheimer approximation breaks down[6] and the electronic states can be coupled with molecular vibrations of proper symmetry, called the JT active modes. In this specific system, the vibrational modes of interest are those of symmetry e and t_2; the total symmetric mode, or breathing mode, produces only a line broadening[16] and is neglected here.

In this paper we consider different vibronic models for JT interaction both on Γ_5 and on Γ_4 multiplets with phonons of symmetry e and t_2. The total Hamiltonian comprises an electronic part, a vibrational part H_v, and a coupling part $H_{JT,e}$ and H_{JT,t_2} for e modes and t_2 modes, respectively. The electronic part includes spin-orbit terms, crystalline field, and molecular exchange field. The vibrational Hamiltonian is taken in elastic approximation and written in a second quantization notation where a displacement is proportional to the sum of creation and annihilation operators. Let us indicate with $H_{v,e}$ and H_{v,t_2} the vibrational Hamiltonians for interacting modes of symmetry e and t_2, respectively. They take the form

$$H_{v,e}(\Gamma_i) = \hbar\omega_e(a_\theta^\dagger a_\theta + a_\epsilon^\dagger a_\epsilon + 1)P_{\Gamma_i}, \tag{2}$$

$$H_{v,t_2}(\Gamma_i) = \hbar\omega_{t_2}\left(a_x^\dagger a_x + a_y^\dagger a_y + a_z^\dagger a_z + \frac{3}{2}\right)P_{\Gamma_i}, \tag{3}$$

where Γ_i is for Γ_4 or Γ_5, P_{Γ_i} is the projector on the electron-spin eigenfunctions belonging to Γ_i multiplet, and $\hbar\omega_e$ and $\hbar\omega_{t_2}$ are the phonon energy for the modes e and t_2, respectively.

The JT interaction Hamiltonian with a mode of e symmetry can be written as

$$H_{JT,e}(\Gamma_i) = \hbar\omega_e\sqrt{S_e(\Gamma_i)}\sum_{k=\theta,\epsilon}[(a_k^\dagger + a_k)D_k(\Gamma_i)], \tag{4}$$

where $S_e(\Gamma_i)$ is the Huang-Rhys factor or the JT energy in unit of the phonon energy, $D_\theta(\Gamma_i)$ and $D_\epsilon(\Gamma_i)$ are the Clebsh-Gordon coefficient matrices expressed on the basis of the electron functions belonging to the multiplet Γ_i and tabulated by Koster *et al.*[14]

For the t_2 mode the JT interaction Hamiltonian becomes

$$H_{JT,t_2}(\Gamma_i) = \hbar\omega_{t_2}\sqrt{S_{t_2}(\Gamma_i)}\sum_{k=x,y,z}[(a_k^\dagger + a_k)D_k(\Gamma_i)], \tag{5}$$

where the D matrices and the S constants have the same meaning as before. All the previous Hamiltonians are understood as multiplied by the identity in the spin space.

In a two-mode vibronic model the vibrational and the interaction Hamiltonians are of course the sum of the vibrational and interaction Hamiltonians corresponding to each mode involved in the model considered, having eventually different symmetry, frequency, and strength of the coupling.

III. CALCULATION PROCEDURE

The Hilbert space for the system in study is given by 14 electron-spin functions partners of the irreducible representations Γ_6, Γ_8, Γ_7, Γ_8', Γ_7' and by the vibrational states $|n_\theta, n_\epsilon\rangle$ or $|n_x, n_y, n_z\rangle$ for one-mode interaction model; and $|n_\theta, n_\epsilon, n_x, n_y, n_z\rangle$ or $|m_x, m_y, m_z, n_x, n_y, n_z\rangle$ for a two-mode interaction model. Here n_θ, n_ϵ, ... label the occupation numbers for the partners of the phonon modes considered. So when the electron-phonon interaction model becomes more complex and a larger number of phonons must be taken into account, one arrives fastly to matrices of a too large dimension to be handled with traditional technique. In Table I we show the dimension of the matrix Hamiltonian at increasing number of phonons for each mode considered.

Luckily the JT matrices are in a sparse form and the Lanczos-recursion method can be efficiently followed to calculate the vibronic eigenstates. For convenience we resume here the main points of the Lanczos-recursion procedure. For

TABLE I. Dimension of the total Hamiltonian at different number of phonons for each interaction model; $N_{e,t_2}(\Gamma_i)$ indicates the total number of vibrational quanta taken in the vibrational states for e and t_2 coupling on Γ_i multiplet.

$N_e(\Gamma_4)$	$N_e(\Gamma_5)$	$N_{t_2'}(\Gamma_4)$	$N_{t_2'}(\Gamma_5)$	$N_{t_2''}(\Gamma_4)$	$N_{t_2''}(\Gamma_5)$	N
1	1	0	0	0	0	126
3	3	0	0	0	0	1400
5	5	0	0	0	0	6174
0	0	1	1	0	0	224
0	0	3	3	0	0	5600
0	0	5	5	0	0	43904
0	0	1	1	1	1	3584
0	0	3	3	3	3	$\sim 10^6$
0	0	5	5	5	5	$\sim 10^8$

more details see, for instance, Refs. 12 and 17. Essentially the method consists in a progressive building of orthonormal states for a tridiagonal representation of a given operator, in our case the Hamiltonian of the vibronic system. Let $|\phi_0\rangle$, $|\phi_1\rangle, \ldots, |\phi_\nu\rangle$ denote the first $\nu+1$ normalized functions of the Lanczos chain; the $|\Phi_{\nu+1}\rangle$ (unnormalized) function is constructed through the three-term recursion relation

$$|\Phi_{\nu+1}\rangle = H|\phi_\nu\rangle - a_\nu|\phi_\nu\rangle - b_\nu|\phi_{\nu-1}\rangle . \tag{6}$$

The next pair of parameters $b^2_{\nu+1}$ and $a_{\nu+1}$ are given, respectively, by the normalization of $|\Phi_{\nu+1}\rangle$ and by the expectation value of the Hamiltonian on it. In the new basis $|\phi_\nu\rangle$ the Hamiltonian operator is represented by a tridiagonal matrix T_M, which is then diagonalized, and whose elements a_ν and b_ν are known up to the order M of the iteration performed. One of the major advantages of the Lanczos procedure is that the lower eigenstates, usually those of interest, are obtained diagonalizing a tridiagonal matrix of rank much lesser than the original one.[17]

The eigenvectors are of course expressed on the basis of the chain states $|\phi_\nu\rangle$ and are in the form

$$|\Psi_n\rangle = \sum_\nu c_{n,\nu}|\phi_\nu\rangle , \tag{7}$$

where the coefficients $c_{n,\nu}$ are provided by the diagonalization of T_M. Usually, for memory reason, in the three term relation (6) one does not store all the vectors $|\phi_\nu\rangle$, and to obtain explicitly the eigenvectors $|\Psi_n\rangle$ the states $|\phi_\nu\rangle$ have to be regenerated by a second Lanczos procedure with the same initial seed state (two-pass Lanczos).[18] Let us remember that a crucial point to efficiently use the Lanczos-recursion procedure is the choice of the initial state of the Lanczos chain. In principle whatever linear combination of the basis functions can be used, but a suitable choice of the seed state can greatly simplify the calculations.[12]

One of the quantities to be calculated here is the partial differential cross section that can be put in the following form in dipole approximation and cubic symmetry:[15,19]

$$\frac{d^2\sigma}{d\Omega d\omega}\frac{k_i}{k_f} = \frac{1}{2}\left(\frac{\gamma e^2}{m_e c^2} g_J\right)^2 F^2(\mathbf{Q}) \sum_{m,n} \rho_n |\langle\Psi_m|J_z|\Psi_n\rangle|^2 \times \delta(E_m - E_n - \hbar\omega). \tag{8}$$

Here $|\Psi_n\rangle$, $|\Psi_m\rangle$ are the vibronic states involved in the transitions, J_z is the component of the total angular momentum perpendicular to the scattering vector $\mathbf{Q}$, $\mathbf{k}_i$ and $\mathbf{k}_f$ are initial and final neutron wave vectors, $F(\mathbf{Q})$ is the magnetic form factor, ρ_n is the Boltzmann population factor of the state $|\Psi_n\rangle$, $\hbar\omega$ is the neutron energy transfer [$\hbar\omega = \hbar^2/2m(k_f^2 - k_i^2)$].

Usually the experiments are performed at small $\mathbf{Q}$ where $F^2(\mathbf{Q}) \simeq 1$. So the key ingredient in the differential cross section (8) remains the matrix elements modulus squared $|\langle\Psi_m|J_z|\Psi_n\rangle|^2$, which requires the knowledge of the vibronic functions $|\Psi_m\rangle$ and $|\Psi_n\rangle$. In principle, they could be evaluated through a two-pass Lanczos worked out for all the states of interest. However, taking advantage of the freedom in the choice of the seed state of the recursion, a faster and manageable procedure is provided in the following.

Let $|\Psi_n\rangle$ be the vibronic starting state for the transitions in study and already determined by a two-pass Lanczos. To obtain the matrix element of interest it is convenient to choose as initial state of the new Lanczos procedure

$$|\phi_0\rangle = \frac{J_z|\Psi_n\rangle}{\sqrt{\langle\Psi_n|J_z^2|\Psi_n\rangle}}, \tag{9}$$

which is the projected state through J_z and normalized. The matrix element becomes

$$\langle\Psi_m|J_z|\Psi_n\rangle = \langle\Psi_m|\phi_0\rangle\sqrt{\langle\Psi_n|J_z^2|\Psi_n\rangle}. \tag{10}$$

Then the differential cross section is immediately given by means of $|c_{m,0}|^2$, that is, the projection modulus squared on the initial state of the Lanczos chain of the vibronic states of interest $|\Psi_m\rangle$ and their reconstruction is so avoided.

Alternatively, it is possible (and convenient when a large number of recursion is needed) to consider the continued fraction expansion of the diagonal Green function matrix element $G_{00}(E)$, whose coefficients are given by the coefficients a_ν and b_ν^2 of the Lanczos chain.[10] The poles of the continued fraction give the eigenvalues of the vibronic system and their residua give the projected density of states which is immediately related to the differential cross section.

As regards the calculation of the magnetic moment let us recall that

$$\langle\boldsymbol{\mu}\rangle = -g_J \sum_n \rho_n \langle\Psi_n|\boldsymbol{J}|\Psi_n\rangle. \tag{11}$$

At the temperature of the experimental measurements,[4,5] below the Néel temperature, only few lower vibronic levels are in practice involved, so the magnetic moment can be directly calculated once the vibronic states $|\Psi_n\rangle$ are determined, entering in the differential cross section calculations.

IV. RESULTS

We have analyzed different vibronic models with electrons interacting with distortions of symmetry e and t_2. Since the JT coupling has been considered acting on the multiplets Γ_4 and Γ_5 simultaneously, in the next we refer to the systems $(\Gamma_4+\Gamma_5)\otimes e$, $(\Gamma_4+\Gamma_5)\otimes t_2$ (one-mode models) and $(\Gamma_4+\Gamma_5)\otimes(t_2'+t_2'')$ (two-mode model).

For each model the functions are allowed to span a vibronic space including up to a total number N of vibrational quanta for each vibronic interaction. Stability of the solution was tested with respect to N and we required energy differences less than 0.5% going from N to $N+1$. In practice the maximum total number of phonon needed has been $N=5$.

The calculations have been carried out in the framework of the Lanczos recursion procedure as illustrated before. The numerical instabilities of this technique due to the finite arithmetic precision of the computers are well known as well as the remedies proposed.[20] Here we have performed a suitable number of overrecursions in such a way to obtain stable eigenstates. When the number of overrecursion to determine the vibronic excited states was too high (of the order of thousands), we have constructed the continued fraction expansion of the ground-state Green's function $G_{00}(E)$, as specified in preceeding section.

A. $(\Gamma_4+\Gamma_5)\otimes e$ interaction model

We have obtained the vibronic levels of Pr^{4+} ion considering the JT interaction Hamiltonian $H_{JT,e}$ described in Sec. II and using the same phonon energy and coupling constant for the JT interaction both on Γ_4 and Γ_5 multiplets. We have first followed the behavior of vibronic energy levels at different JT energies $(0<S_e<1)$ and at different values of $\hbar\omega_e$ in the range 10–60 meV. To our knowledge, there are no phonon dispersion curves available for PrO_2, however, the experimental spectra[1] suggest energies of effective phonon modes within that range.

Looking at the energies and at the peak intensities of the vibronic levels obtained we have noticed two main transitions shifted by about 130 meV and identified, for $S_e\to 0$, with the E_0 and E_1 levels (see Sec. II). In the middle we have found a lot of vibronic levels, but only two having a not negligible peak intensity. They are shifted by about 10 meV and 25 meV from the first line, and in the next we will call these intermediate vibronic levels E_{int}' and E_{int}'', respectively.

We have seen that the energy of the phonon mode influences the energy separation of E_{int}' and E_{int}'' levels from the first transition, while the JT energy influences, particularly, the peak intensity of the transitions. However, whatever phonon energies and coupling strengths are considered in the calculations, the relative peak intensities (to respect the main transition) of the intermediate vibronic states are of the order of 10^{-2}, too weak to be compared with the experimental spectra.

We must then discard the e modes as the only or main responsible mode for JT coupling in this system.

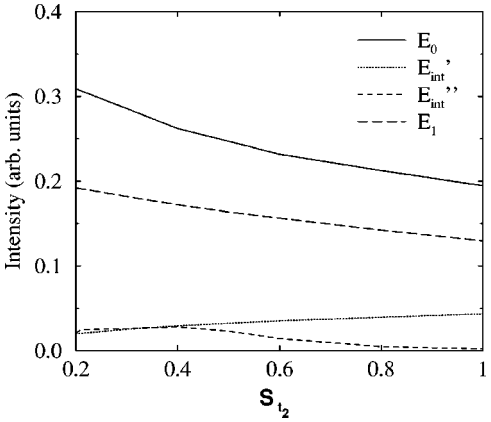

FIG. 2. Peak intensities in arbitrary units of the lower vibronic levels as a function of S_{t_2}; $\hbar\omega_{t_2}=30$ meV.

B. $(\Gamma_4+\Gamma_5)\otimes t_2$ interaction model

The results presented here are obtained considering the JT interaction Hamiltonian H_{JT,t_2} described in Sec. II. As before the energy of the t_2 phonon mode has been changed in the range 10–60 meV, and the behavior of the vibronic energy levels are followed as the Huang-Rhys factor S_{t_2} is growing from zero until $S_{t_2}=1$ $[S_{t_2}(\Gamma_4)=S_{t_2}(\Gamma_5)]$. In this case also we can obtain two main lines separated by about 130 meV, many intermediate vibronic levels and among them only two have significant intensity. We continue to call them E_{int}' and E_{int}''. These intermediate vibronic levels are always weak, but the relative peak intensity is larger by one order of magnitude to respect the previous model. In Fig. 2 we show how the peak intensities of E_0, E_1, E_{int}', and E_{int}'' are influenced by the strength of the phonon coupling. To construct this figure we have taken $\hbar\omega_{t_2}=30$ meV and $S_{t_2}(\Gamma_4)=S_{t_2}(\Gamma_5)$.

Then we have tried different values for $S_{t_2}(\Gamma_4)$ and $S_{t_2}(\Gamma_5)$, looking particularly to the intensities of the intermediate levels. The best agreement with the experimental differential cross section is obtained with $S_{t_2}(\Gamma_4)=0.42$ and $S_{t_2}(\Gamma_5)=0.22$.

The differential cross section calculated taking the magnetic form factor equal to one, is reported in Figs. 3 and 4. In Fig. 3 we report the energies and the peak intensities of the transitions; in Fig. 4 we show a superposition of intensities using Lorentzian line shapes with half-width taken from the experimental spectra as indicated in the figure caption. Notice the presence of a shoulder at about 160 meV, in agreement with the experimental results. Of course a phonon frequency only cannot give results covering completely the observed scattering band.

Then, without any other adjustment of the parameters, we have calculated the magnetic moment considering, here and in the next, $\boldsymbol{\mu}$ directed along (1,1,1). We have found $|\boldsymbol{\mu}|=0.83\mu_B$, a value smaller than that calculated without vibronic coupling ($|\boldsymbol{\mu}|=1.02\mu_B$), but always larger than the experimental ones.[4,5]

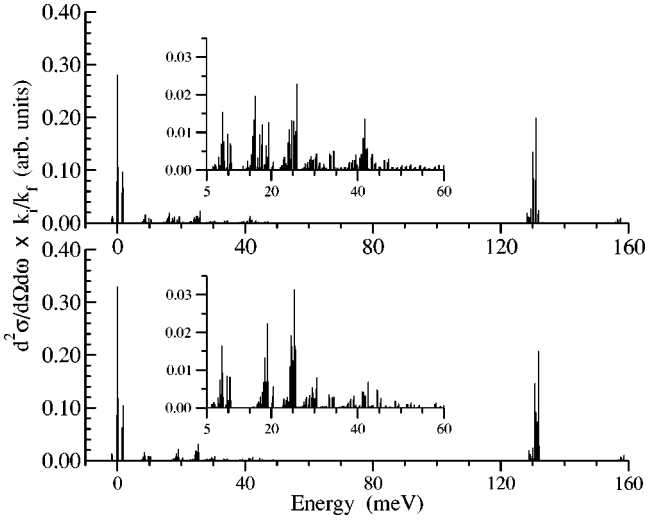

FIG. 3. Peak intensities (in arbitrary units) and energies of the calculated spectra for a one-mode t_2 model (bottom) and a two-mode t_2 model (top). In the insets the details due to transitions to the excited vibronic levels in the energy range 5–60 meV are shown. The parameters used are indicated in the text.

C. $(\Gamma_4+\Gamma_5)\otimes(t_2'+t_2'')$ interaction model

In this case the Hamiltonian includes the contribution of two phonon modes of t_2 symmetry, but having different energies and different coupling strengths. Fixed at the best values found in the preceeding section the phonon energy and the coupling strength for the first mode, we have studied the effect of the second mode, taking the phonon energy always in the range 10–60 meV. As expected a more rich structure is found between the E_0 and E_1 levels, particularly in the range 10–20 meV and near to 40 meV. In Fig. 3 (top) and in Fig. 4 (solid line) the calculated differential cross section for an interaction model with two distortions of t_2 symmetry is shown. The phonon energies and the coupling strength have been $\hbar\omega_{t_2'}=30$ meV, $S_{t_2'}(\Gamma_4)=0.42$, $S_{t_2'}(\Gamma_5)=0.22$, $\hbar\omega_{t_2''}$ $=60$ meV, $S_{t_2''}(\Gamma_4)=0.01$, and $S_{t_2''}(\Gamma_5)=0.15$. The crystal-field parameters have been adjusted to fix at 130 meV the energy separation between the two main transitions, but this is not the main concern here. As it can be seen, the agreement with the experimental spectra[1] is more satisfactory here than in the previous interaction model, even if the coupling strength for the second phonon mode is weak. Looking at these results we think that a dynamical JT effect with many frequencies is really responsible of the broad structure found in the measured spectra. Within this model we have calculated also the differential cross section in a wider range of energies, around 340 meV and 730 meV, where there is experimental information.[1] The experimental spectra exhibit transitions not well resolved around 340 meV and 360 meV, then a broad peak centered at about 730 meV. The calculations agree satisfactorily with the experimental results, as can be seen from Fig. 5, where we show the energies and the peak intensities of the main transitions with superposed Lorentzian line shapes having half-width roughly corresponding to the experimental ones. However, some comments are needed. The spectrum calculated in the energy range 330–370 meV corresponds to the transitions from the ground vibronic level of Γ_8 symmetry to excited vibronic levels of symmetry Γ_6 and Γ_8 and the contribution of many excited vibronic levels is evident looking at Fig. 5, left side. Instead a less rich structure is found in the energy range 700–750 meV, (right side of Fig. 5), because the corresponding transitions are towards excited levels of Γ_7 symmetry, on which the JT effect is much less important.

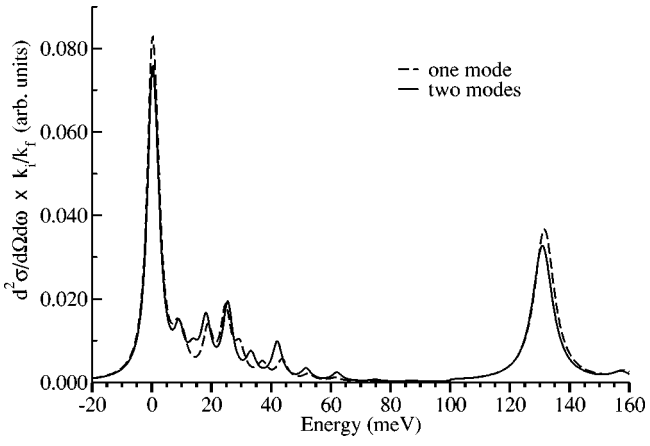

FIG. 4. Calculated spectra in arbitrary units for a one-mode t_2 model (dashed line) and two-mode t_2 model (solid line). Half-width for Lorentzian line shapes is 2 meV for the first few lines and 4 meV for lines after 100 meV. The other parameters are the same as in Fig. 3.

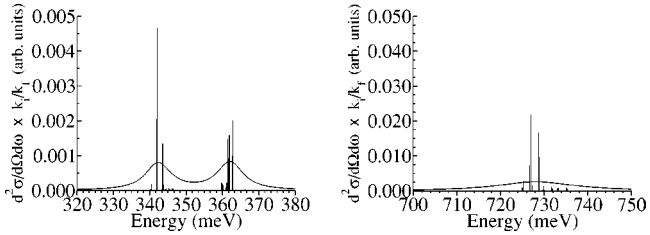

FIG. 5. Calculated spectra around 340 meV (left side) and 730 meV (right side) for a two-mode t_2 model. The peak intensities are given in arbitrary units. Half-widths for the Lorentzian line shapes are 4 meV and 10 meV, respectively.

In the end we have calculated the magnetic moment using the same set of parameters given above. We have obtained $|\boldsymbol{\mu}|=0.73\mu_B$, in very good agreement with recent measurements on single crystals.[5]

V. CONCLUSIONS

We have exploited the adaptability of the Lanczos recursion procedure to calculate with high precision the vibronic levels of Pr^{4+} ions on PrO_2 dioxides. The choice suggested here for the initial state of the Lanczos procedure has allowed us to easily calculate the differential cross section to be compared with neutron spectroscopy measurements. Then the magnetic moment has been directly evaluated. Different vibronic models have been analyzed here, one-mode model and two-mode model, with phonons of e and t_2 symmetry.

The results obtained indicate that t_2 distortions are more important than e distortions and a two-mode vibronic model better agrees with the experimental results. The knowledge of PrO_2 phonon dispersion curves should be greatly advantageous to more strictly define the vibronic model, as well as the knowledge of the coupling constants calculated by first principles and their behavior at different temperature. Very recently Gardiner *et al.*[21] have found interesting temperature effects in the measured lattice parameters that should also be reflected in the calculation of the coupling constants and in the nature of the ground vibronic state at low temperature. In the literature there are examples of vibronic systems having the ground state with symmetry and degeneracy different from the starting orbital state for a certain range of parameters.[22–24] Work is in progress to explore this possibility in our models too. Moreover the results presented in the same paper[21] suggest the presence of cooperative JT effects. In our paper the interaction among different JT centers at different sites is not taken into account, but it should be a natural evolution of our models and calculation procedure.

[1] A.T. Boothroyd, C.H. Gardiner, S.J.S. Lister, P. Santini, B.D. Rainford, L.D. Noailles, D.B. Currie, R.S. Eccleston, and R.I. Bewley, Phys. Rev. Lett. **86**, 2082 (2001).

[2] S. Kern, F. Trouw, C.-K. Loong, and G.H. Lander, J. Appl. Phys. **67**, 4830 (1990).

[3] J. Dabrowski, V. Zavodinsky, and A. Fleszar, Microelectronics Reliability **41**, 1093 (2001).

[4] S. Kern, C.-K. Loong, and G.H. Lander, Phys. Rev. B **32**, 3051 (1985); S. Kern, C.-K. Loong, J. Faber, and G.H. Lander, Solid State Commun. **49**, 295 (1984).

[5] C.H. Gardiner, A.T. Boothroyd, S.J.S. Lister, M.J. McKelvy, S. Hull, and B.H. Larsen, Appl. Phys. A: Mater. Sci. Process. **A74**, S1773 (2002).

[6] I.B. Bersuker and V.Z. Polinger, *Vibronic Interactions in Molecules and Crystals*, Springer Series in Chemical Physics (Springer-Verlag, Berlin, 1989).

[7] I.B. Bersuker, *Electronic Structures and Properties of Transition Metal Compounds* (Wiley-Interscience, New York, 1996).

[8] C. Lanczos, J. Res. Natl. Bur. Stand. **45**, 255 (1950); **49**, 33 (1952); *Applied Analysis* (Prentice-Hall, Englewood Cliffs, NJ, 1956).

[9] R. Haydock, V. Heine, and M.J. Kelly, J. Phys. C **5**, 2845 (1972); **8**, 2591 (1975); see also D.W. Bullet, R. Haydock, and M.J. Kelly, in *Solid State Physics*, edited by H. Erhenreich, F. Seitz, and D. Turnbull (Academic, New York, 1980), Vol. 35.

[10] G. Grosso and G. Pastori Parravicini, Adv. Chem. Phys. **62**, 81 (1985); **62**, 133 (1985).

[11] M.C.M. O'Brien and S.N. Evangelou, J. Phys. C **13**, 611 (1980); Solid State Commun. **36**, 29 (1980); M.C.M. O'Brien, J. Phys. C **16**, 85 (1983); **16**, 6345 (1983); **18**, 4963 (1985).

[12] L. Martinelli, M. Passaro, and G. Pastori Parravicini, Phys. Rev. B **39**, 13 343 (1989).

[13] O. Mualin, E.E. Vogel, M.A. de Orúe, L. Martinelli, G. Bevilacqua, and H.-J. Schulz, Phys. Rev. B **65**, 035211 (2001); G. Bevilacqua, L. Martinelli, and E.E. Vogel, *ibid.* **66**, 155338 (2002).

[14] G.F. Koster, J.O. Dimmock, R.G. Wheeler, and H. Statz, *Properties of the Thirty-Two Point Groups* (MIT University Press, Cambridge, MA, 1963).

[15] D. Ippolito, Thesis, University of Pisa, 2002.

[16] G. Bevilacqua, L. Martinelli, and G. Pastori Parravicini, J. Phys.: Condens. Matter **10**, 10 347 (1998).

[17] G. Grosso and G. Pastori Parravicini, *Solid State Physics* (Academic Press, London, 2000), p. 185 and references therein.

[18] H.Q. Lin and J.E. Gubernatis, Comput. Phys. **7**, 400 (1993).

[19] W. Marshall and S. W. Lovesey, *Theory of Thermal Neutron Scattering* (Oxford University Press, Oxford, UK, 1971); S.W. Lovesey, *Theory of Thermal Neutron Scattering from Condensed Matter* (Oxford University Press, Oxford, UK, 1884).

[20] J.C. Cullum and R.A. Willoughby, *Lanczsos Algorithms for Large Symmetric Eigenvalue Computations* (Birkhauser, Boston, 1985), Vols. I and II.

[21] C.H. Gardiner, A.T. Boothroyd, P. Pattison, M.J. McKelvy, G.J. McIntyre, and S.J.S. Lister, cond-mat/0311294 (unpublished).

[22] M.C.P. Moate, M.C.M. O'Brien, J.L. Dunn, C.A. Bates, Y.M. Liu, and V.Z. Polinger, Phys. Rev. Lett. **77**, 4362 (1996).

[23] H. Koizumi and I.B. Bersuker, Phys. Rev. Lett. **83**, 3009 (1999); H. Koizumi, I.B. Bersuker, J.E. Boggs, and V.Z. Polinger, J. Chem. Phys. **112**, 8470 (2000).

[24] G. Bevilacqua, I.B. Bersuker, and L. Martinelli, in *Vibronic Interactions: Jahn-Teller Effect in Crystals and Molecules*, edited by M.D. Kaplan and G.O. Zimmerman (Kluwer Academic, The Netherlands, 2001), pp. 229–233.